

# Effects of growth hormone treatment on growth plate, bone, and mineral metabolism of young rats with uremia induced by adenine

Déborá Claramunt<sup>1</sup>, Helena Gil-Peña<sup>2</sup>, Rocío Fuente<sup>1</sup>, Enrique García-López<sup>2</sup>, Olaya Hernández Frías<sup>1</sup>, Flor A. Ordoñez<sup>2</sup>, Julián Rodríguez-Suárez<sup>2</sup> and Fernando Santos<sup>2</sup>

**BACKGROUND:** In a model of growth retardation secondary to chronic kidney disease (CKD) induced by adenine, this study explores the effects of growth hormone (GH) therapy on growth plate and mineral metabolism.

**METHODS:** Weaning female rats receiving a 0.5% adenine diet during 21 days, untreated (AD) or treated with GH (ADGH) for 1 week, were compared with control rats receiving normal diet, either *ad libitum* or pair-fed with AD animals. AD and ADGH rats had similarly elevated serum concentrations of urea nitrogen, parathyroid hormone (PTH), and fibroblast growth factor 23 (FGF23).

**RESULTS:** Uremia induced by adenine caused growth retardation and disturbed growth cartilage chondrocyte hypertrophy. We demonstrated marked expression of aquaporin 1 in the growth plate, but its immunohistochemical signal and the expression levels of other proteins potentially related with chondrocyte enlargement, such as Na-K-2Cl cotransporter, insulin-like growth factor 1 (IGF-1), and IGF-1 receptor, were not different among the four groups of rats. The distribution pattern of vascular endothelial growth factor was also similar. AD rats developed femur bone structure abnormalities analyzed by micro-computerized tomography.

**CONCLUSION:** GH treatment accelerated longitudinal growth velocity, stimulated the proliferation and enlargement of chondrocytes, and did not modify the elevated serum PTH or FGF23 concentrations or the abnormal bone structure.

**G**rowth impairment is a major manifestation of chronic kidney disease (CKD) of pediatric age onset. The pathogenesis of growth retardation is multifactorial, including low infant size at birth, anorexia and nutritional deficits, cachexia, anemia, chronic inflammation, metabolic acidosis, renal bone disease, and hormonal disturbances (1,2). CKD causes partial resistance of peripheral tissues to growth hormone (GH) and insulin-like growth factor 1 (IGF-1) actions (3,4), but treatment with high, pharmacological doses of GH results in acceleration of growth rate and improved adult height (5).

The growth plate of long bones, including the epiphyseal growth cartilage and the adjacent metaphyseal primary spongiosa, is the organ where longitudinal endochondral growth takes place. As the study of growth plate is extremely difficult in children, young uremic rodents are used to investigate growth plate alterations induced by CKD. The abnormalities of growth cartilage structure and dynamics, as well as the effects of GH therapy on these alterations, which are able to accelerate growth rate, have been described in 5/6 nephrectomized rats (6). Our group has recently characterized the histomorphometric changes of the epiphyseal cartilage in a model of CKD-induced growth retardation in young rats made uremic by intake of a diet containing adenine. In comparison with the 5/6 nephrectomy, in the adenine model of CKD the surgical stress is avoided, the renal damage is potentially reversible, at least in early stages, and the degree of achieved glomerular filtration rate reduction is more uniform (7,8).

Despite the fact that the growth plate of rats treated with adenine has been shown to be smaller than that of control pair-fed rats, whereas 5/6 nephrectomy usually causes expansion of the growth cartilage, the height of the distal hypertrophic chondrocytes is reduced in comparison with normal renal function rats, in both types of CKD models, induced by either subtotal nephrectomy or adenine (7,9). This finding is consistent with the known observation that longitudinal growth rate in mammals is mostly dependent on the enlargement of epiphyseal cartilage hypertrophic chondrocytes, a process that recent investigations have shown to occur through three sequential phases: true cell hypertrophy, cell swelling, and a final period of hypertrophy regulated by local IGF-1 (10). The mechanisms underlying growth plate chondrocyte volume increase, and hence bone lengthening, are poorly understood. Bush *et al.* (11) showed that Na<sup>+</sup>, K<sup>+</sup>, 2Cl<sup>-</sup> cotransporter (NKCC1) mRNA is expressed in the hypertrophic zone of the growth plate. NKCC1 might have an important role in the process of hypertrophic chondrocyte volume increase. Similarly, although the presence of aquaporin 1 (AQP1), a

<sup>1</sup>Department of Medicine, Universidad de Oviedo, Asturias, Spain; <sup>2</sup>Department of Pediatrics, Hospital Universitario Central de Asturias, Oviedo, Spain. Correspondence: D. Claramunt (declata@gmail.com)

Received 19 October 2016; accepted 15 March 2017; advance online publication 26 April 2017. doi:10.1038/pr.2017.95

**Table 1.** Serum biochemical determinations reflecting renal function and mineral metabolism in the four groups of rats ( $n=5$  per group)<sup>a</sup>

	Creatinine (mg/dl)	Urea nitrogen (mg/dl)	Calcium (mg/dl)	Phosphate (mg/dl)	Intact PTH (pg/ml)	FGF23 (pg/ml)
C	$<0.2 \pm 0.0$	$14 \pm 1$	$10.8 \pm 0.2$	$8.6 \pm 0.2$	$84 \pm 17$	$317 \pm 30$
AD	$0.6 \pm 0.1^b$	$70 \pm 6^b$	$10.9 \pm 0.3$	$10.7 \pm 0.7^b$	$480 \pm 31^b$	$361 \pm 60$
ADGH	$0.6 \pm 0.1^b$	$59 \pm 8^b$	$11.4 \pm 0.3$	$10.7 \pm 0.6^b$	$501 \pm 51^b$	$436 \pm 80$
PF	$<0.2 \pm 0.0^{c,d}$	$16 \pm 1^{c,d}$	$11.4 \pm 0.5$	$8.0 \pm 0.4^{c,d}$	$67 \pm 7.2^{c,d}$	$170 \pm 35^{b,c,d}$

AD, 0.5% adenine diet; ADGH, 0.5% adenine diet and GH treatment; C, normal diet; FGF23, fibroblast growth factor 23; PF, normal diet pair-fed with the AD group; PTH, parathyroid hormone

<sup>a</sup>Values are mean  $\pm$  SEM.

<sup>b</sup>Compared with the control group,  $P < 0.05$ .

<sup>c</sup>Compared with the AD group,  $P < 0.05$ .

<sup>d</sup>Compared with the ADGH group,  $P < 0.05$ .

member of the aquaporin (AQP) family of membrane-spanning water channels responsible for the rapid transport of water across the plasma membrane, has not been demonstrated in the growth plate (12), it may be hypothesized that AQP1 may be involved in the volume expansion of hypertrophic chondrocytes.

The present study was carried out in young rats with growth impairment secondary to adenine-induced CKD to ascertain (a) the immunohistochemical local expression of proteins likely involved in the process of chondrocyte enlargement and chondrocyte maturation, and (b) the effects of GH therapy on the growth plate, which have not been reported so far in this animal model. We hypothesized that growth retardation of this experimental model of CKD would be associated with changes in both the morphology of the growth plate and in the expression of the analyzed proteins. We also assumed that these abnormalities might be reversed by GH treatment.

## RESULTS

### Renal Function and Mineral Metabolism

As shown in **Table 1**, the groups receiving adenine diet (AD) and adenine diet with GH treatment (ADGH) had similar degrees of renal failure and secondary hyperparathyroidism. AD and ADGH rats had higher serum fibroblast growth factor 23 (FGF23) levels than pair-fed (PF) rats, with the three groups consuming the same amount of phosphorus.

### Growth and Nutrition

Data on growth and food intake of the four groups of animals are shown in **Table 2**. The AD animals were growth retarded as demonstrated by lower length gain and growth velocity, assessed by osseous front advance, compared with the PF and *ad libitum* control groups (C). GH treatment of AD rats (ADGH group) improved body weight, accelerated growth velocity, and increased food efficiency (**Table 2** and **Figure 1a**).

### Growth Plate Histomorphometry

There were differences in the heights of the growth cartilages and the hypertrophic zones among the groups of animals (**Table 3** and **Figure 1b**). Growth retardation of AD rats was associated with less proliferating chondrocytes (**Table 3** and

**Figure 1c**) and with a reduced height of the terminal chondrocytes in comparison with C and PF groups (**Table 3**). GH treatment increased the height of the most distal chondrocytes, as well as the cell proliferation rate (**Table 3** and **Figure 1**).

### Immunohistochemistry

As for the proteins potentially involved in the process of chondrocyte enlargement (NKCC1, AQP1, IGF-1, and IGF-1 receptor (IGF-1R)), the pattern of distribution was similar in the four groups of rats, with the immunohistochemical signal being cytoplasmic and particularly strong in the hypertrophic stratum of the growth plate (**Figure 2**). Vascular endothelial growth factor (VEGF) was also expressed in the hypertrophic chondrocytes in the four groups of animals, although the intensity of the signal looked weaker at the osteochondral junction level in the AD group compared with the other groups. The number of cells positively marked for VEGF was not different among the four groups of rats (C  $61.1 \pm 9.5\%$ ; AD  $59.9 \pm 19.4\%$ ; ADGH  $66.6 \pm 13.1\%$ ; PF  $61.3 \pm 5.2\%$ ).

### Bone Structure

**Table 4** shows the variables measured by micro-computed tomography (microCT) in the rats' femurs. Abnormalities found in the AD and ADGH groups consisted essentially in lower trabecular thickness, increased cortical porosity, and accelerated bone turnover (BS/BV). No significant differences were found between AD and ADGH groups in any of the measured parameters.

## DISCUSSION

In a rat model of growth retardation secondary to uremia induced by adenine, this study provides novel information on the growth plate expression of proteins potentially involved in this process of chondrocyte enlargement in CKD and reports the effects of GH treatment as well. The process of chondrocyte enlargement has been shown to take place through three sequential phases: true cell hypertrophy, cell swelling, and a final period of hypertrophy regulated by local IGF-1 (10).

To find out whether the phase of chondrocyte swelling may be disturbed in CKD, the immunohistochemical distribution of transporters and channels regulating water and electrolyte

**Table 2.** Growth and nutrition in the four groups of rats (*n* = 5 per group)<sup>a</sup>

	Weight gain (g)	Length gain (cm)	Food intake (g)	Food efficiency <sup>b</sup> (g/g)	Osseous front advance (µm/day)
C	112.6 ± 4.7	11.1 ± 0.3	406 ± 10	0.17 ± 0.01	293 ± 16
AD	63.3 ± 4.8 <sup>c</sup>	7.2 ± 0.2 <sup>c</sup>	257 ± 9 <sup>c</sup>	0.05 ± 0.02 <sup>c</sup>	141 ± 13 <sup>c</sup>
ADGH	77.7 ± 7.0 <sup>c,d</sup>	7.4 ± 0.5 <sup>c</sup>	269 ± 11 <sup>c</sup>	0.26 ± 0.01 <sup>d</sup>	257 ± 18 <sup>c,d</sup>
PF	60.0 ± 3.8 <sup>c,e</sup>	8.1 ± 0.3 <sup>c,d</sup>	257 ± 9 <sup>c</sup>	0.08 ± 0.03 <sup>c,e</sup>	251 ± 10 <sup>c,d</sup>

AD, 0.5% adenine diet; ADGH, 0.5% adenine diet and GH treatment; C, normal diet; PF, normal diet pair-fed with the AD group.

<sup>a</sup>Values are mean ± SEM.

<sup>b</sup>Food efficiency was calculated as grams of gained weight divided by grams of consumed food.

<sup>c</sup>Compared with the control group, *P* < 0.05.

<sup>d</sup>Compared with the AD group, *P* < 0.05.

<sup>e</sup>Compared with the ADGH group, *P* < 0.05.

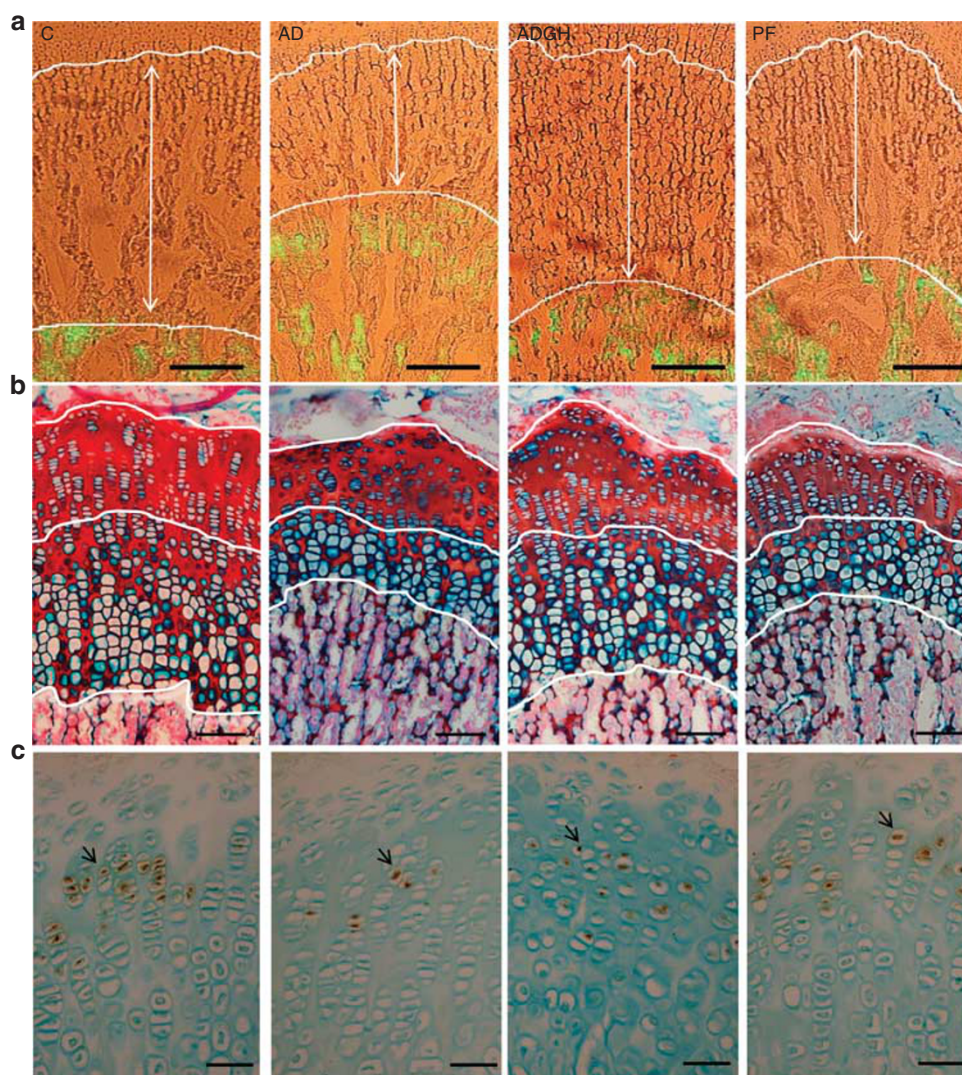


**Figure 1.** Growth plates of control (c), Adenine 0.5% (AD), adenine 0.5% treated with GH (ADGH), and pair-fed (PF) rats. Representative sections of each group are shown. **(a)** Osseous front advance: the mean distance between the metaphyseal end of the growth cartilage and the fluorescent calcein front indicates longitudinal bone growth rate during the last 5 days of the study. Bars = 500 µm. **(b)** Histological appearance of growth plates stained by alcian blue/safranin. Bars = 100 µm. **(c)** Proliferative activity of chondrocytes, as assessed by bromodeoxyuridine labeling. Bars: 50 µm.

traffic through the cell membrane was analyzed. Water channels facilitate plasma membrane water permeability to the levels required for efficient coupling between NaCl

transport and water transport in epithelia that carry out isosmotic fluid transport (13). AQP1 is a widely expressed water channel, whose physiological function has been most

**Table 3.** Histological characteristics of the proximal femur growth plate cartilage in the four groups of rats ( $n=5$  per group)<sup>a</sup>

	Height ( $\mu\text{m}$ )	Hypertrophic zone height ( $\mu\text{m}$ )	Terminal chondrocyte height ( $\mu\text{m}$ )	BrdU labeling (per 100 cells)
C	438.0 $\pm$ 20.1	220.9 $\pm$ 16.4	26.2 $\pm$ 1.9	38 $\pm$ 2
AD	366.0 $\pm$ 19.6 <sup>b</sup>	191.4 $\pm$ 19.0	21.7 $\pm$ 2.3 <sup>b</sup>	30 $\pm$ 2 <sup>b</sup>
ADGH	493.3 $\pm$ 54.5 <sup>c</sup>	316.9 $\pm$ 52.4 <sup>c</sup>	25.3 $\pm$ 2.2 <sup>c</sup>	47 $\pm$ 2 <sup>c</sup>
PF	310.0 $\pm$ 19.5 <sup>b,c,d</sup>	149.5 $\pm$ 7.7 <sup>b,c,d</sup>	23.9 $\pm$ 1.3 <sup>b,c</sup>	42 $\pm$ 3 <sup>c</sup>

AD, 0.5% adenine diet; ADGH, 0.5% adenine diet and GH treatment; BrdU, 5-bromo-2'-deoxy-uridine; C, normal diet; PF, normal diet pair-fed with the AD group.

<sup>a</sup>Values are means  $\pm$  SEM.

<sup>b</sup>Compared with the control group,  $P < 0.05$ .

<sup>c</sup>Compared with the AD group,  $P < 0.05$ .

<sup>d</sup>Compared with the ADGH group,  $P < 0.05$ .

thoroughly characterized in the kidney. AQP1 has also been found in other human tissues, such as red blood cells, vascular endothelium, the gastrointestinal tract, sweat glands, and lungs (12). Interestingly, we demonstrated for the first time the expression of AQP1 in growth plate chondrocytes, mostly in the hypertrophic zone. It is tempting to speculate that AQP1 may have a significant role in the enlargement of the hypertrophic chondrocytes. There were no noticeable changes in the pattern of distribution of AQP1 and NKCC1 in the rats receiving adenine. As for NKCC1, the importance of this membrane cotransporter in the process of chondrocyte enlargement has been demonstrated (11). However, no studies were available in uremia.

The volume enlargement of epiphyseal cartilage hypertrophic chondrocytes is the most important factor that determines growth rate in mammals' long bones (14). The study presented here confirms previous findings indicating that uremia interferes with the process of chondrocyte enlargement (9,15), as demonstrated by the smaller size of the terminal chondrocytes in AD compared with those in PF rats. This adverse effect of CKD on growth was potentiated by an additional inhibitory effect of uremia on the proliferative chondrocyte activity, another factor that influences the growth rate, although less importantly.

The effects of GH therapy in rats made uremic by adenine intake have not been reported so far. This study shows that, in this experimental model, GH given at doses known to cause the maximum effect on growth of 5/6 nephrectomized young rats (16) exerted an anabolic action, shown by the increase in food efficiency and the subsequent amelioration of weight gain. In addition, GH administration accelerated growth rate as a result of stimulating the proliferation of growth cartilage chondrocytes and reversing the inhibiting action of uremia on the process of maturation and enlargement of chondrocytes. It is noteworthy that, although GH treatment resulted in a higher osseous front advance rate in the ADGH group compared with the AD group, the snout-tail length was not different between these two groups of animals, likely because GH was administered for 1 week only. Longer periods of administration would be necessary to appreciate differences in whole-body length (6).

The animal model of CKD presented here resulted in secondary hyperparathyroidism, elevated FGF23 concentrations, and alterations in bone structure, analyzed by microCT,

in agreement with the increased bone fragility found in adult uremic rats (17,18). GH treatment, although it did accelerate longitudinal growth rate, did not induce further significant changes in serum PTH or FGF23 concentrations and did not improve bone mineral density and bone mass, likely because the period of administration was not long enough (19,20) or only the effect of GH treatment is not sufficient. Troib *et al.* (21) showed that the combination of GH (2 weeks) and exercise therapy improved bone volume and the number of trabeculae—an effect not achieved when the rats were treated only with GH.

The beneficial effect of GH administration on growth was not associated with changes in the immunohistochemical pattern of NKCC1, AQP1, IGF-1, or IGF-1R. Neither the distribution of these proteins nor the intensity of the signal were modified, indicating that their local expression at the growth cartilage was not influenced by GH treatment, at least when assessed by immunohistochemistry. Further studies using more sensitive techniques might be necessary to detect quantitative variations in the analyzed proteins.

VEGF-mediated vascularization is an essential signal to regulate growth plate morphogenesis through the induction of coupling resorption of cartilage with bone formation. The results of the inhibition of VEGF activity have shown impaired bone formation and the expansion of hypertrophic chondrocytes, along with an almost complete suppression of blood vessel invasion (22). CKD has been associated with a decrease in growth plate (VEGF) mRNA and immunostainable VEGF levels (23). In our study, the signal of VEGF in the distal portion of the hypertrophic zone looked weaker in the chondrocytes adjacent to the osteochondral junction in the AD group, and the intensity of the signal was normalized by GH treatment (ADGH rats). However, the intensity of the immunohistochemical signal is not a good parameter to reflect mild–moderate differences in the tissue expression of a protein and we could not appreciate differences in the number of marked cells. Thus, our results do not allow confirming that growth plate VEGF expression was inhibited in this uremia model and stimulated by GH.

In conclusion, in rats with adenine-induced CKD that caused growth retardation associated with secondary hyperparathyroidism and elevated FGF23, this study discloses the growth plate expression of proteins likely related with the process of chondrocyte enlargement, which is known to be

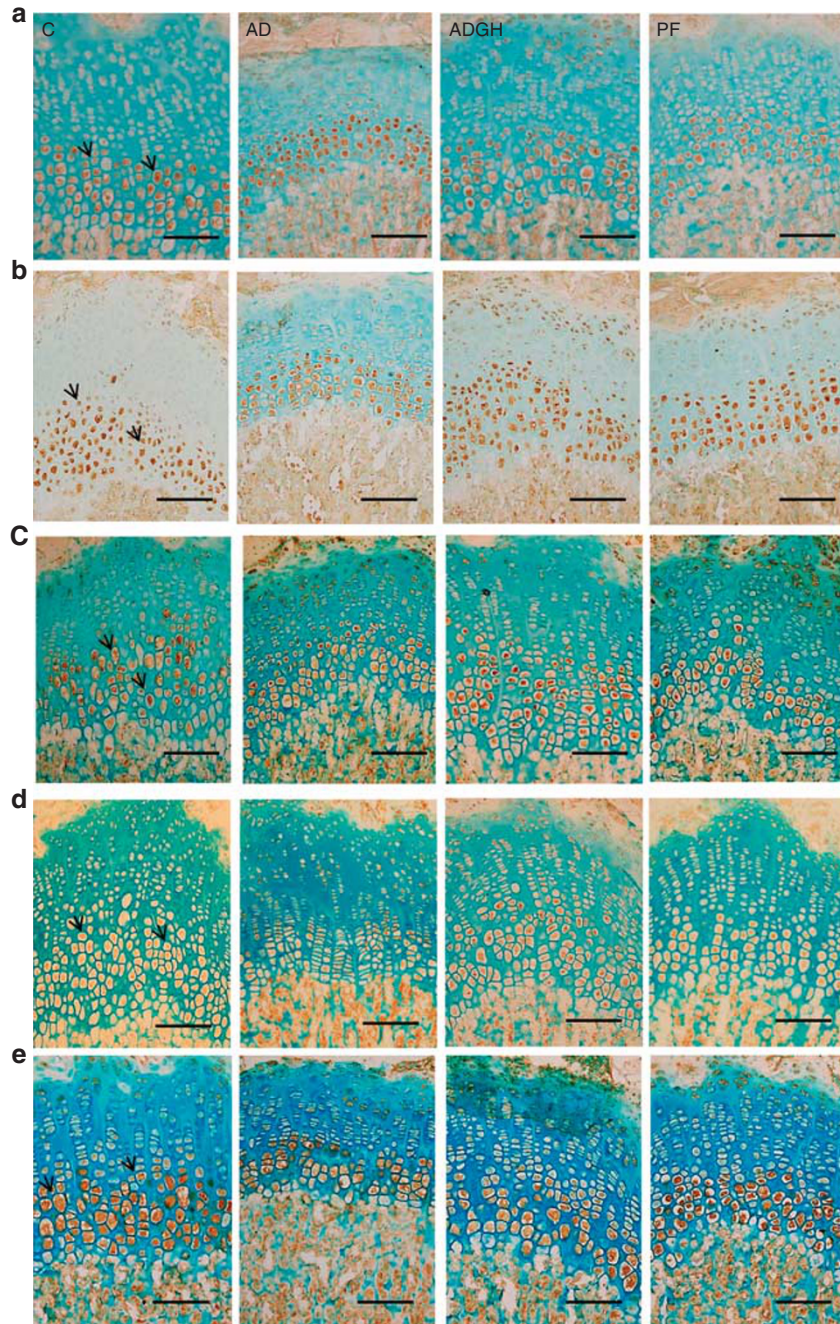


**Figure 2.** Immunohistochemical signals in the growth plate of control (C), Adenine 0.5% (AD), Adenine 0.5% treated with GH (ADGH), and pair-fed (PF) groups. Representative images are shown for (a) Na-K-2Cl cotransporter (NKCC1), (b) aquaporin 1 (AQP1), (c) insulin-like growth factor 1 (IGF-1), (d) IGF-1 receptor (IGF-1R), and (e) vascular endothelial growth factor (VEGF). Bars = 100 μm.

crucially linked to growth rate. In addition, the study provides novel information on the effects of GH treatment on growth, growth plate, and mineral metabolism in this experimental model.

**METHODS**

Female Sprague–Dawley rats aged 3 weeks and weighing 65 ± 5 g (Charles River Laboratories, L’Arbresle, France) were housed in individual cages under controlled conditions of light (12 light/dark cycles) and temperature (21–23 °C). Rats’ diets were purchased from

Ssniff Spezialdiäten GmbH (Soest, Germany) (reference number V1534). Diet contained 1% calcium, 0.7% phosphorus, 19% protein, 1 IU/g vitamin D, and adenine 0.5%. All animals had free access to tap water. The study complied with current legislation on animal experiments in the European Union and was approved by the Ethics Committee on Animal Research of the University of Oviedo, Spain.

**Experimental Protocol and Sample Collection**

After 3 days of adaptation, the animals were classified into four groups: C (normal diet); AD (0.5% adenine diet); ADGH (0.5% adenine diet and GH treatment); and PF (normal diet, pair-fed with

**Table 4.** Bone architecture analyzed by microCT in the four groups of rats ( $n=6$  per group)<sup>a</sup>

	C	AD	ADGH	PF
BV/TV (%)	25.1 ± 1.3	27.1 ± 1.5	25.3 ± 1.8	27.7 ± 0.8
TbN (1/mm)	6.3 ± 0.3	7.1 ± 0.4	7.0 ± 0.4	6.8 ± 0.3
Tb.Sp (mm)	0.10 ± 0.01	0.09 ± 0.01	0.09 ± 0.01	0.10 ± 0.01
Tb.Th (mm)	0.040 ± 0.001	0.038 ± 0.001 <sup>b</sup>	0.036 ± 0.001 <sup>b</sup>	0.041 ± 0.001 <sup>c, d</sup>
BS/BV	90 ± 1.3	94.8 ± 1.7 <sup>b</sup>	100.8 ± 4.3 <sup>b</sup>	85.7 ± 0.7 <sup>b, c, d</sup>
Tt.Ar (mm <sup>2</sup> )	32.4 ± 2.2	28.6 ± 1.7	30.2 ± 1.3	31.0 ± 1.9
Ct.Ar (mm <sup>2</sup> )	3.7 ± 0.3	3.2 ± 0.1	3.4 ± 0.2	3.5 ± 0.1
Ct.Ar/Tt.Ar (%)	10.8 ± 0.7	11.3 ± 0.5	11.2 ± 0.6	11.5 ± 0.6
Ct.Th (mm)	0.51 ± 0.07	0.40 ± 0.01	0.39 ± 0.02	0.44 ± 0.01
Ct.Po (%)	1.1 ± 0.2	3.5 ± 0.3 <sup>b</sup>	3.5 ± 0.5 <sup>b</sup>	1.3 ± 0.2 <sup>c, d</sup>

AD, 0.5% adenine diet; ADGH, 0.5% adenine diet and GH treatment; BS/BV, bone surface/volume ratio; BV/TV, bone volume/tissue volume; C, normal diet; Ct.Ar, cortical area; Ct.Ar/Tt.Ar, cortical area/total area; Ct.Po, cortical porosity; Ct.Th, cortical thickness; PF, normal diet pair-fed with the AD group; Tb.Sp, trabecular separation; Tb.Th, trabecular thickness; TbN, trabecular number; Tt.Ar, total area inside periosteum.

<sup>a</sup>Values are mean ± SEM.

<sup>b</sup>Compared with the control group,  $P < 0.05$ .

<sup>c</sup>Compared with the AD group,  $P < 0.05$ .

<sup>d</sup>Compared with the ADGH group,  $P < 0.05$ .

AD group) (7). Recombinant human GH (rhGH) (Norditropin, Novo Nordisk Pharma, Madrid, Spain) was administered intraperitoneally to the ADGH group from day 14 to day 20 of the protocol at a dosage of 3.3 mg/kg/day, given at 0900 hours and 1700 hours (16). The other groups received solvent following identical protocol of administration.

Animals were killed by exsanguination under anesthesia with ketamine (4 mg per 100 g weight; Ketolar, Pfizer, Madrid, Spain) and thiopental sodium (1.25 mg per 100 g weight; Penthotal, Abbot, Madrid, Spain) on day 21 of the protocol. Five days before killing, each animal received 30 mg/kg calcein (Sigma, St. Louis, MO) by intraperitoneal route for calculation of the osseous front advance as an index of longitudinal bone growth rate (24). Bromodeoxyuridine (BrdU; 100 mg/kg; Sigma-Aldrich, Madrid, Spain) was injected intraperitoneally 1, 9, and 17 h before death. Blood samples were collected and stored at  $-20^{\circ}\text{C}$  until biochemical measurements. Rights femurs were removed and the proximal ends fixed and embedded in methyl methacrylate, as previously described (6). Left femurs were fixed in 40% ethanol and used for analysis of calcein labeling, BrdU immunohistochemistry, and micro-scanner evaluation. Right femurs were fixed in 4% paraformaldehyde (PFA) for histomorphometric analysis.

### Blood Biochemistry

Serum concentrations of creatinine, urea nitrogen, calcium, and phosphate were measured by an autoanalyzer Kodak EktachemR (Eastman Kodak, Rochester, NY). Intact parathormone (PTH) levels were determined by enzyme-linked immunosorbent assay (ELISA kit; Immunotopics, San Clemente, CA). FGF23 levels were measured by ELISA (Kainos Laboratories, Tokyo, Japan).

### Growth and Nutrition

Food intake and body weight were measured daily using an electronic balance (Ohaus GT 2100, Florham Park, NJ). Food efficiency was calculated as the ratio between weight gained and food consumed (g/g) by each animal between days 14 and 21 of the protocol. Nose to tail-tip length was measured under anesthesia on days 0 and 21. Longitudinal growth rate was measured in 10- $\mu\text{m}$ -thick frontal sections of the proximal end of femurs obtained using a rotary microtome (HM355S, Microm, Barcelona, Spain) fitted with tungsten carbide blades. Sections were examined under an Olympus incident light fluorescence microscope (Olympus BX41, Olympus Optical, Barcelona, Spain) coupled to a digital camera (Olympus

DP11, Olympus Optical) to detect calcein label. Images were captured and the distance between the chondro-osseous junction and the calcein label was measured using the software Osteo versión 13.2.6 (Bioquant Image Analysis Corporation, Nashville, TN). The mean value of these measurements divided by 5 (days) was considered the osseous front advance per day, representing the daily longitudinal bone growth rate in each animal.

### Growth Plate Histology and Histomorphometry

Frontal sections (5  $\mu\text{m}$  thick) of proximal femurs fixed in PFA were stained with alcian blue/safranin for morphometric analysis. Heights of the growth cartilage and its hypertrophic zone were identified following morphological criteria and measured at regular intervals in two slides per animal using the image analysis system described above (6). Height of the three most distal hypertrophic chondrocytes was measured in alternate columns using the same system.

### Immunohistochemistry

Immunodetection of BrdU, IGF-1, IGF-1R, AQP1, NKCC1, and VEGF was performed as described elsewhere (6). Two sections were analyzed per animal, and the proliferating activity was expressed as the number of positive cells per 100 cells in the proliferative zone, previously defined as the band of tissue between the resting zone and a line traced by the most distal BrdU-labeled cells. The immunohistochemistry techniques were performed in 5- $\mu\text{m}$ -thick sections of the proximal end of the femur fixed in PFA. After deplastication in acetone and rehydration, all sections were treated with hydrogen peroxide and goat serum, VEGF for 75 min, 2 h NKCC1, IGF-1, and IGF-1R for 1:30 h (diluted 1:4 in PBS, pH 7.4, Sigma), except AQP1 which did not require pretreatment to unmask antigens. Thereafter, sections were incubated overnight at  $4^{\circ}\text{C}$  with a 1/20 dilution of polyclonal anti-VEGF antibody (Novus Biologicals, Littleton, CO), 1/20 dilution of anti-NKCC1 (Abcam, Cambridge, UK), 1/10 dilution of anti-IGF-I (MyBioSource, San Diego, CA), 1/5 dilution of anti-IGF-1R (Santa Cruz, Dallas, TX), and 1/100 dilution of anti-AQP1 (Abcam, Cambridge, UK). After 30 min of incubation with anti-rabbit or anti-mouse secondary conjugated antibody (EnVision; Dako Diagnostics), the final reaction product was revealed with diaminobenzidine, and methyl green was used as a counterstain. VEGF immunohistochemical signal was measured in the chondrocytes of the hypertrophic zone and expressed as number of positive cells per 100 hypertrophic chondrocytes.

### Bone Structure

The region of proximal metaphysis to mid-diaphysis of all femurs was scanned by high-resolution microCT SkyScan 1174 (Bruker, Kontich, Belgium). The images obtained during scanning were reconstructed using the software NRecon (Bruker). For morphometric analysis, the software provided by the manufacturer was used. For the analysis of the trabecular region, a total of 225 slices were selected (75 for primary and 150 for secondary spongiosa) and adaptive grayscale threshold levels between 0.37 and 1.62 g/cm<sup>3</sup> of bone mineral density were used. For the diaphysis cortical region 125 slices were chosen. In all cases, the growth plate was chosen as the point of reference. Global grayscale threshold levels for this area were between 0.53 and 1.62 g/cm<sup>3</sup> of bone mineral density.

The following morphometric parameters were measured: bone volume fraction, trabecular thickness, trabecular number, trabecular separation, and turnover for the trabecular area. For the cortical region, the following parameters were measured: total cross-sectional area inside the periosteal envelope, cortical bone area, cortical area fraction, cortical thickness, and cortical porosity (Ct.Po; %). The parameters were measured according to the ASBMR histomorphometry nomenclature (25).

### Statistical Analysis

Values are given as mean ± standard error of the mean (SEM). Differences between groups were assessed by ANOVA followed by the Student–Newman–Keuls method. For two group comparisons, Student's *t* test was used. A *P* value ≤ 0.05 was considered indicative of significant difference. All data sets were analyzed using SPSS 15.0 (SPSS, Chicago, IL).

### ACKNOWLEDGMENTS

We gratefully thank Teresa Usín for expert technical assistance.

### STATEMENT OF FINANCIAL SUPPORT

This study has been partially supported by the University of Oviedo, FEDER funds, ISC III FIS PI12-00987, Fundación Bancaria CajAstur, and Fundación Nutrición y Crecimiento.

Disclosure: The authors declare no conflict of interest.

### REFERENCES

1. Mahesh S, Kaskel F. Growth hormone axis in chronic kidney disease. *Pediatr Nephrol* 2008;23:41–8.
2. Mencarelli F, Kiepe D, Leozappa G, Stringini G, Cappa M, Emma F. Growth hormone treatment started in the first year of life in infants with chronic renal failure. *Pediatr Nephrol* 2009;24:1039–46.
3. Tönshoff B, Kiepe D, Ciarmatori S. Growth hormone/insulin-like growth factor system in children with chronic renal failure. *Pediatr Nephrol* 2005;20:279–89.
4. Tönshoff B, Veldhuis JD, Heinrich U, Mehls O. Deconvolution analysis of spontaneous nocturnal growth hormone secretion in prepubertal children with preterminal chronic renal failure and with end-stage renal disease. *Pediatr Res* 1995;37:86–93.
5. Seikaly MG, Salhab N, Gipson D, Yiu V, Stablein D. Stature in children with chronic kidney disease: analysis of NAPRTCS database. *Pediatr Nephrol* 2006;21:793–99.
6. Molinos I, Santos F, Carbajo-Perez E, et al. Catch-up growth follows an abnormal pattern in experimental renal insufficiency and growth hormone treatment normalizes it. *Kidney Int* 2006;70:1955–61.
7. Claramunt D, Gil-Peña H, Fuente R, et al. Chronic kidney disease induced by adenine: a suitable model of growth retardation in uremia. *Am J Physiol Renal Physiol* 2015;309:57–62.
8. Shuvy M, Nyska A, Beeri R, et al. Histopathology and apoptosis in an animal model of reversible renal injury. *Exp Toxicol Pathol* 2011;63:303–6.
9. Cobo A, Carbajo E, Santos F, García E, López JM. Morphometry of uremic rat growth plate. *Miner Electrolyte Metab* 1996;22:192–5.
10. Cooper KL, Oh S, Sung Y, Dasari RR, Kirschner MW, Tabin CJ. Multiple phases of chondrocyte enlargement underlie differences in skeletal proportions. *Nature* 2013;495:375–8.
11. Bush PG, Pritchard M, Loqman MY, Damron TA, Hall AC. A key role for membrane transporter NKCC1 in mediating chondrocyte volume increase in the mammalian growth plate. *J Bone Miner Res* 2010;25:1594–603.
12. Bondy C, Chin E, Smith BL, Preston GM, Agre P. Developmental gene expression and tissue distribution of the CHIP28 water-channel protein. *Proc Natl Acad Sci USA* 1993;90:4500–4.
13. Knepper MA. The aquaporin family of molecular water channels. *Proc Natl Acad Sci USA* 1994;91:6255–8.
14. Breur GJ, VanEnkevort BA, Farnum CE, Wilsman NJ. Linear relationship between the volume of hypertrophic chondrocytes and the rate of longitudinal bone growth in growth plates. *J Orthop Res* 1991;9:348–59.
15. Santos F, Fernández Fuente M, Carbajo E. The growth plate in chronic renal insufficiency. *Nefrologia* 2003;23:18–22.
16. Kovacs GT, Oh J, Kovacs J, et al. Growth promoting effects of growth hormone and IGF-I are additive in experimental uremia. *Kidney Int* 1996;49:1413–21.
17. De Schutter TM, Neven E, Persy VP, et al. Vascular calcification is associated with cortical bone loss in chronic renal failure rats with and without ovariectomy: the calcification paradox. *Am J Nephrol* 2011;34:356–66.
18. Ferrari GO, Ferreira JC, Cavallari RT, et al. Mineral bone disorder in chronic kidney disease: head-to-head comparison of the 5/6 nephrectomy and adenine models. *BMC Nephrol* 2014;15:69.
19. Allen DB, Fogo A, el-Hayek R, Langhough R, Friedman AL. Effects of prolonged growth hormone administration in rats with chronic renal insufficiency. *Pediatr Res* 1992;31:406–10.
20. Bechtold S, Dalla Pozza R, Schwarz HP, Simon D. Effects of growth hormone treatment in juvenile idiopathic arthritis: bone and body composition. *Horm Res* 2009;72:60–4.
21. Troib A, Guterman M, Rabkin R, Landau D, Segev Y. Endurance exercise and growth hormone improve bone formation in young and growth-retarded chronic kidney disease rats. *Nephrol Dial Transplant* 2016;31:1270–9.
22. Gerber H, Vu T, Ryan A, Kowalski J, Werb Z, Ferrara N. VEGF couples hypertrophic cartilage remodeling, ossification and angiogenesis during endochondral bone formation. *Nat Med* 1999;5:623–8.
23. Troib A, Landau D, Kachko L, Rabkin R, Segev Y. Epiphyseal growth plate growth hormone receptor signaling is decreased in chronic kidney disease-related growth retardation. *Kidney Int* 2013;84:940–9.
24. Alvarez-Garcia O, Carbajo-Pérez E, García E, et al. Rapamycin retards growth and causes marked alterations in the growth plate of young rats. *Pediatr Nephrol* 2007;22:954–61.
25. Bouxsein ML, Boyd SK, Christiansen BA, Guldberg RE, Jepsen KJ, Müller R. Guidelines for assessment of bone microstructure in rodents using micro-computed tomography. *J Bone Miner Res* 2010;25:1468–86.